Journal of Physics: Conference Series **500** (2014) 172005 doi:10.1088/1742-6596/500/17/172005

From laminar to turbulent detonations in energetic materials from molecular dynamics simulations

Vasily V Zhakhovsky[1], Mikalai M Budzevich[1], Aaron C Landerville[1], Ivan I Oleynik[1] and Carter T White[2]

[1]University of South Florida, 4202 East Fowler Avenue, Tampa, Florida 33620-5700, USA
[2]Naval Research Laboratory, Washington DC 20375-5320, USA

E-mail: 6asi1z@gmail.com

Abstract. The structure of a self-sustained detonation wave in solid energetic materials was studied using molecular dynamics simulations. Energetic materials are described by the AB model with parameters modified to investigate the detonation-wave structures. It is found that depending on the reaction barrier for the exothermic reactions driving the detonation and the boundary conditions of the sample this simple model exhibits a detonation structure that can range from a planar to a complex turbulent detonation. The different regimes of condensed-phase detonation seen are similar to those observed in gases and diluted liquids.

1. Introduction

A detonation charges through an explosive gas or a condensed-phase energetic material (EM) as a shock wave that causes the exothermic chemical reactions that sustain it. Although successful in estimating detonation speeds, the classic Zel'dovich, von Neumann, and Doering (ZND) detonation theory [1–3] is intrinsically one-dimensional (1D) and hence cannot capture the more complex non-planar detonation structures that have been observed in gases [3–5]. Such structures can arise from instabilities in a metastable planar detonation on the verge of failure. Rather than collapsing, however, the planar detonation spontaneously evolves into much more complex structures that allow the detonation to proceed. Embedded in these structures are high temperature and pressure regions, where key chemical reactions are initiated that would be much less favored in the corresponding ZND detonation, where temperatures and pressures are lower. In particular, the temperatures and pressures in these extreme regions are noticeably higher than those predicted by ZND theory in the von Neumann (vN) spike of the corresponding planar detonation [3]. Although well known in gases, such complex structures have not yet been observed experimentally in detonating solids due to difficulties in the characterization of EM's subjected to ultrafast energy release in the presence of extreme pressures and temperatures at the much smaller length scales appropriate for materials. Because of these fundamental challenges, atomistic molecular dynamics (MD) simulations, such as described in this paper, provide an attractive alternative for investigating the conditions that can lead to such structures in EM's. Indeed, we find that a variant of the well-known AB Model of perhaps the simplest possible detonating material can not only support a planar detonation but also much more complex structures that parallel known gas-phase behavior depending on the choice of parameters and sample size.


Content from this work may be used under the terms of the Creative Commons Attribution 3.0 licence. Any further distribution of this work must maintain attribution to the author(s) and the title of the work, journal citation and DOI.
Published under licence by IOP Publishing Ltd

2. Model and methods

Our starting point is the AB Model that has proven successful in reproducing the major features of a classic ZND detonation in large-scale condensed-phase MD simulations [6, 7]. This model is based on reactive empirical bond order (REBO) potentials with parameters chosen not to fit a particular system but rather to yield a simple generic model of an explosive—a diatomic molecular solid composed of AB molecules that when shocked can undergo endothermic chemical reactions along chemically reasonable reaction pathways to form more stable A_2 and B_2 products. In this work, following Heim *et al.* [8], we have used a variant of the original AB model that allows the reaction barrier E_b for the half reactions, $A + AB \rightarrow A_2 + B + 3\,eV$ and $B + BA \rightarrow B_2 + A + 3\,eV$ to be easily modified. It is these exothermic reactions that potentially drive the detonation. This modification to the model is accomplished while maintaining chemically reasonable potential energy surfaces for these half reactions with the transition state occurring along the minimum energy pathway in a collinear geometry with an early barrier to reaction as is illustrated in figure 1.

Our modified version of the AB Model is a bit different than Heim's, but the same idea is used to adjust E_b, which allows the chemistry to be altered without otherwise changing the key features of the model. A full description of the REBO potentials used to obtain the results reported below is given elsewhere [9]. Also found there is a description of the long-range interactions used to bind the AB molecules into a molecular solid.

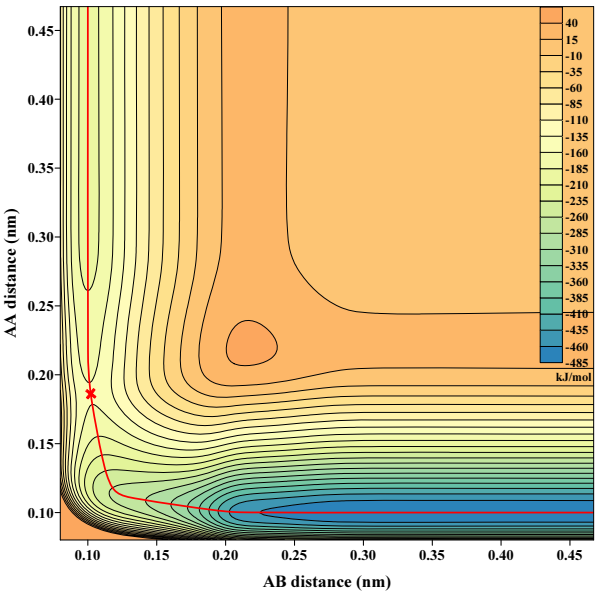


Figure 1. 2D map of potential energy for the linear three-atom system AAB. The reaction pathway for $A + AB \rightarrow A_2 + B$ is indicated by a red line. The position of the transition state giving $E_b = 0.36\,eV$ is shown by an X on the reaction pathway.

The simulations using the REBO potentials were implemented using a moving window (MW) MD method [10, 11] that decouples time and length scales in MD simulations. In this approach the shock wave structure is simulated in the reference frame moving with the detonation front. Unreacted material is fed into the simulation box upstream from the detonation front and reacted material is removed downstream at the other end of the simulation box. Chemical reactions are started at the onset of the simulation by a short range potential barrier of finite height applied at the downstream boundary. Once a detonation begins the barrier is removed. Because the removal of atoms takes place in the rarefaction tail of reactants beyond the sonic point, any perturbations at the left boundary cannot affect the shock front and reaction zone.

MD simulations of detonations in AB solids with different reaction barriers were started in a sample with longitudinal dimension $L_x = 200\,nm$ and small transverse dimensions, $L_y = 8.1\,nm$ and $L_z = 7.8\,nm$. The longitudinal direction x corresponds to the direction of propagation of the detonation front, with periodic boundary conditions imposed in the transverse directions, y and z. To start simulations of detonations in larger sized samples with either rigid wall or periodic boundary conditions (BC's), we always used the atom positions and velocities obtained after establishment of quasi-steady 1D detonation in this small sample. Such an approach is widely used in computational fluid dynamics to investigate the stability of planar detonations [12].

To analyze the chemical makeup of the detonating AB material, fractions of reactant $\lambda(\mathrm{AB})$ and product molecules $\lambda(\mathrm{A}_2, \mathrm{B}_2)$ are calculated. To decide if a pair of atoms i and j constitute a diatomic molecule, the following criteria are applied: (a) atom i is closest to atom j, and atom j is closest to atom i; (b) the distance between i and j is less than 1.5 times the equilibrium bond distance; and, (c) the sum of the kinetic energies of i and j in the pair's center of mass reference frame and their potential energies is negative. If any of the above criteria are not satisfied for atoms i and j, then they are termed "radicals" and assigned to the radical fraction $\lambda(\mathrm{A}^*, \mathrm{B}^*)$.

3. Laminar detonation

As with earlier versions of the AB model, the present version supports a steady unsupported planar detonation when E_b is small. In such cases, the planar detonation front exhibits all the major features predicted by ZND theory; a shock-wave front with a vN spike where reactions were initiated, followed by a reaction zone and after-shock laminar flow of the reaction products, all of 1D character. In these cases, the detonation velocity D obtained directly from the simulation is also in excellent agreement with D predicted by ZND theory using the equation of state and the Chapman–Jouguet (CJ) condition.

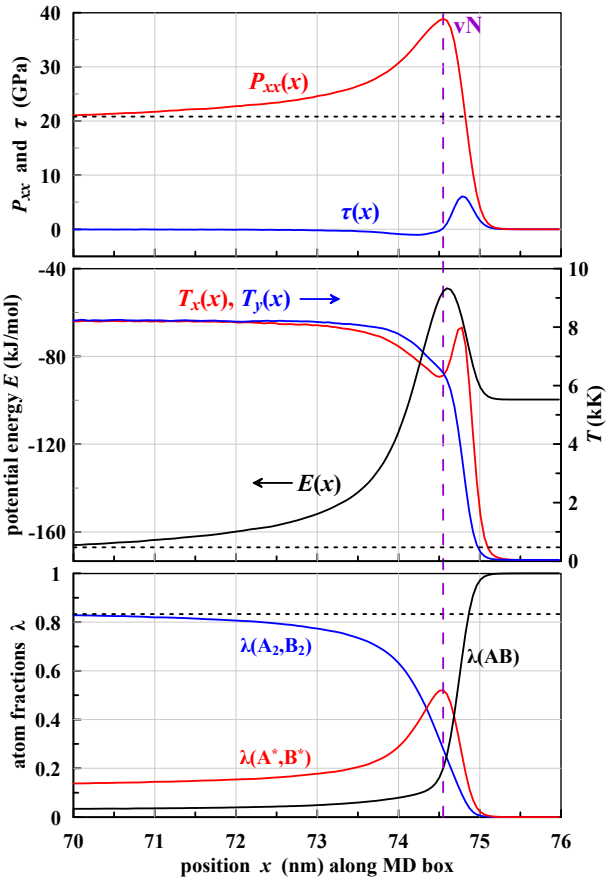


Figure 2. 1D self-sustained laminar detonation wave moving at $D = 7.05$ km/s in the AB model with $E_b = 0.101$ eV. Top panel: pressure P_{xx} and shear stress τ; Middle panel: potential energy per atom $E(x)$, and $T_x(x)$ and $T_y(x)$ components of temperature; Bottom panel: fraction in radicals $\lambda(\mathrm{A}^*, \mathrm{B}^*)$, products $\lambda(\mathrm{A}_2, \mathrm{B}_2)$, and reactants $\lambda(\mathrm{AB})$. Dotted horizontal lines show the corresponding values at the CJ point. Dashed vertical line indicates position of the vN point.

Profiles for the longitudinal component of the pressure tensor $P_{xx}(x)$, shear stress $\tau(x)$, and the potential energy $E(x)$ from an example stable planar detonation with $E_b = 0.101$ eV are given in figure 2. As is typical, D obtained from the simulations in this case, 7.05 km/sec, is within 0.5% of that predicted by ZND theory, 7.02 km/sec. Comparing $E(x)$ and $\tau(x)$ profiles, we see that relaxation of shear stress starts when the pressure reaches half the vN spike in the leading shock front, and is fully completed before the majority of reactions have been started. Increase of the reaction barrier from 0.101 to 0.198 eV resulted in the appearance of nanometer-sized perturbations/ripples, but the 1D planar detonation front remained stable. Moreover, an increase of one transverse dimension of the MD box from 8 nm to 105 nm did not change the 1D nature of the detonation front during 1 ns of simulation.

As the system moves along the Rayleigh line to the vN point at $P = 38.8$ GPa and $T = 6.4$ kK, the chemical composition of the AB material begins to change but remains far from chemical equilibrium. For example, at the vN point $\lambda(\mathrm{AB}) = 0.2$, $\lambda(\mathrm{A}_2, \mathrm{B}_2) = 0.28$, and $\lambda(\mathrm{A}^*, \mathrm{B}^*) = 0.52$ but an equilibrium NVT simulation gives $\lambda(\mathrm{AB}) = 0.009$, $\lambda(\mathrm{A}_2, \mathrm{B}_2) = 0.95$, and $\lambda(\mathrm{A}^*, \mathrm{B}^*) = 0.041$ at the same conditions. The velocity distribution function (VDF) within

the shock front is also far from equilibrium. As a result, the longitudinal "temperature" T_x has a peak that is noticeably higher than the transverse T_y.

The intensive temperature-induced dissociation of AB molecules starts within the shock front when $T_x \sim 3\,\mathrm{kK}$ with the concentration of A* and B* radicals reaching its maximum at the vN point. In the flow following the vN point, the majority of A_2 and B_2 molecules form reaching an equilibrium concentration at the CJ point. Thus, the 1D detonation front can be roughly divided into two zones: a dissociation zone before the vN point where reactants loose their identity and a following association zone where products slowly form.

The atom VDF and potential energy distribution function (EDF) within the dissociation zone and at the vN and CJ points are shown in figure 3. The VDF within the dissociative zone is similar to the bimodal velocity distribution observed in shock-wave simulation of nonreactive gases and liquids [10,13]. Evolution of the obtained VDF across the shock front can be reproduced reasonably well by the Tamm–Mott-Smith bimodal approximation [14]. Collisions between atoms distributed widely in velocity space lead to large momentum transfers and thus dissociation of AB molecules entering the shock front. As a result, the atom potential energy in the EDF broadens from that appropriate for AB molecules towards zero, where the potential energy of free radicals is concentrated. In the association zone between the vN and CJ points reactions lead to A_2 and B_2 molecules, and the EDF begins to spread towards the potential energy of atoms in those molecules. Finally, the EDF and corresponding chemical composition reach an equilibrium state at the CJ point. The local chemical composition remains in equilibrium in the rarefaction flow with slowly decreasing temperature after the CJ point.

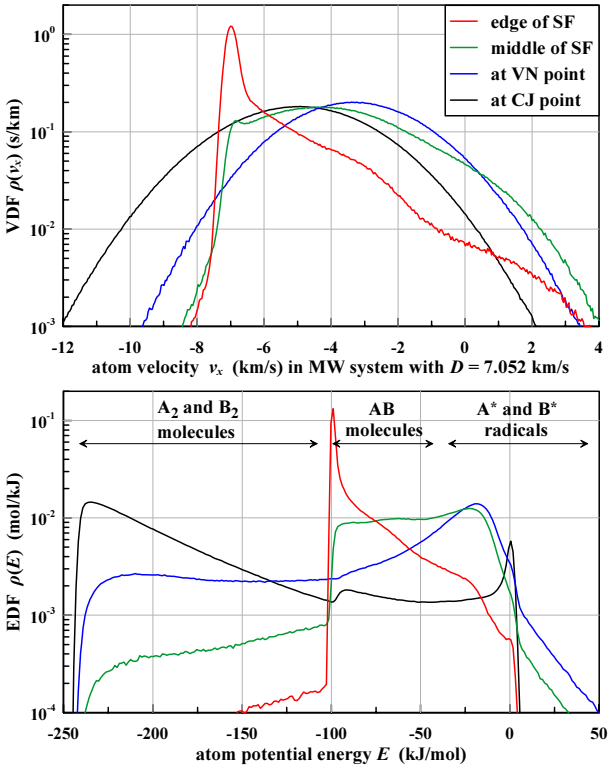


Figure 3. Velocity (top panel) and potential energy (bottom panel) distribution functions, obtained in two thin layers of [74.8,75] nm and [74.6,74.8] nm within a leading shock front, in a layer of [74.4,74.6] nm at the VN, and in a layer [41,43] nm at the CJ point across a detonation wave in the AB model solid with $E_b = 0.101$ eV.

4. 2D cellular and transverse detonations

If the reaction barrier is increased to 0.367 eV in the AB sample with a small transverse cross-section of $8.1\,\mathrm{nm} \times 7.8\,\mathrm{nm}$, the detonation collapses. This happens because the thickness of the reaction zone in the 1D detonation front decreases with increasing E_b to the point that spontaneous pressure/density fluctuation can suppress the pressure in the vN spike resulting in a decrease of the chemical reaction rate and hence a decay of the detonation.

Such longitudinal instabilities can be avoided if the geometrical 1D constraints are removed by increasing the cross-section of the sample, thus allowing the 1D detonation wave to develop into a complex, non-planar detonation front containing "hot" spots with pressures higher than in the corresponding vN spike of the 1D detonation. These hot spots make the detonation almost insensitive to large spontaneous fluctuations. Indeed, once one transverse dimension of the MD box was extended from 8 nm to 32 nm, a complex 2D single-cell detonation regime formed.

Figure 4(a) shows the many-cellular pattern of detonation in an AB solid with periodic BC's and large transverse $y-$dimension of 105 nm. The cross section contains two Mach stems and two detonation cells. The cell length is $\sim$65 nm and the cell height is $L_y/2 = 52.6$ nm. In such a large sample we did not observe the detonation pattern with a larger single cell indicating that the cell height in this AB solid has an upper limit lying between 65 and 105 nm. We also observed a cellular pattern in samples with rigid-wall BC's in the transverse directions. Unlike the sample with rigid-wall BC's, however, we found that as time progressed, the cellular 2D detonation for the sample with periodic BC's suddenly transforms into a transverse detonation pattern produced by collisions of weak incident shock waves and strong oblique and transverse shock waves shown in figure 4(b). Further nano-second simulations confirmed that this three-head transverse detonation pattern remains stable regardless of variations in the pressure amplitudes in neighboring heads.

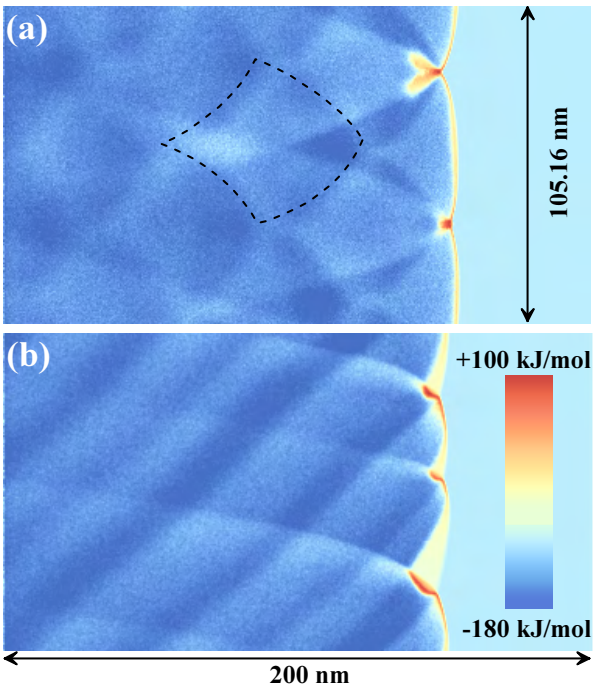


Figure 4. Map of potential energy shows structure of 2D cellular (a) and transverse (b) detonations in an AB solid with $E_b = 0.367$ eV and periodic BC's. The dimensions of the MD simulation box are 200 nm $\times$ 105.2 nm $\times$ 15.6 nm.

The 3 nm net thickness of the 1D planar detonation front in a sample with small transverse dimensions increases to $\sim$50 nm for the 2D detonation patterns shown in figure 4. The strong transverse shocks and Mach stems in the detonation front produced local "hot" spots having pressures much higher than 52 GPa in the vN spike achieved in the corresponding planar, homogeneous detonation front, thus accelerating local chemical reaction rates, and making the detonation insensitive to spontaneous fluctuations.

5. 3D turbulent detonations

A 3D turbulent detonation regime was observed in a large AB sample (y–z transverse dimensions of 105 nm $\times$ 101 nm) with an activation barrier of 0.367 eV. Once the transverse dimensions of the 8.1 nm $\times$ 7.8 nm original sample were increased by a factor of 13, the 1D detonation, originally propagating at a speed of 8.4 km/s, with CJ and vN point pressures of 25 GPa and 52 GPa, respectively, transformed into a turbulent multi-head 3D detonation pattern propagating with almost the same net speed. The transition from the 1D to turbulent regime began with the development of small ripples in the planar front, which appeared within the first several pico-seconds. Then, the ripples grew into non-planar alternating hot and cold zones resulting in an increased net thickness of the detonation front from 3 nm to $\sim$40 nm. The turbulent regime

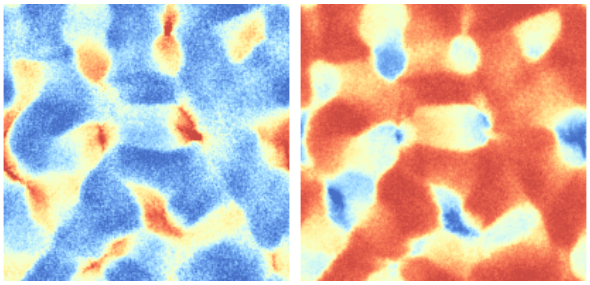


Figure 5. Snapshots of transverse y–z cross sections of the detonation front in an AB solid with energy barrier 0.367 eV. Left and right panels show maps of the potential energy and the product fraction, respectively. Dimensions of the cross sections are 105 nm $\times$ 101 nm.

is characterized by a highly inhomogeneous distribution of pressure in the interval 21 GPa–70 GPa. Figure 5 shows the maps of potential energy and product fraction within a transverse cross-section of the detonation front: the dark blue spots in the energy map correspond to a low pressure of 21 GPa while the bright red spots correspond to pressures up to 70 GPa.

Although the turbulent detonation regime was stable within the time scale of the MD simulation (up to 100 ps), its local dynamics involved the appearance and disappearance of many low- and high-pressure spots. Such phenomena have also been observed experimentally in gases [2, 3], and termed pulsating-turbulent detonations. The 3D turbulent regime produced many high-temperature, high-pressure detonation heads where chemical reactions were ignited. Thus, the heads play the role of conventional hot spots. In contrast to the traditional concept of hot spots in EMs that require the presence of pre-existing defects, the observed hot spots appeared naturally as detonation heads within the turbulent regime of detonation propagation in an AB crystal with a high reaction barrier.

6. Summary

The results reported in this paper establish that even the minimalist AB model of an EM can support incredibly rich detonation structures depending on the choice of parameters and sample sizes. For relatively low reaction barriers, an initially planar detonation front remains stable irrespective of the cross-section of the sample. However, for somewhat higher barriers, the planar detonation front becomes unstable through development of transverse perturbations and begins to decay. This decay, however, can be prevented by increase of one of the transverse dimensions of the sample resulting in a 2D cellular detonation. Such cellular patterns are present in samples with either periodic or rigid-wall BC's in the transverse directions, but samples with periodic BC's can subsequently transform to a 2D transverse detonation. Samples with the same E_b but larger transverse dimensions in both directions can exhibit 3D pulsating-turbulent detonations. Although at a much smaller scale, these different regimes of condensed-phase detonation exhibit structures similar to those observed in gases and diluted liquids.

Acknowledgments

The work at USF and NRL was supported by NRL and ONR, respectively. The work at USF was also supported by the NSF, DTRA, and an USF Research Faculty Pathway grant. Simulations were performed using the NSF XSEDE facilities, the USF Research Computing Cluster, and the computational facilities of the Materials Simulation Laboratory at USF.

References

[1] Zel'dovich Y B and Kompaneets A 1960 *Theory of Detonation* (New York: Academic)
[2] Fickett W and Davis W C 1979 *Detonation* (Berkeley: University of California)
[3] Lee J H S 2008 *The Detonation Phenomenon* (Cambridge: Cambridge University Press)
[4] Duff R E and Knight H T 1952 *J. Chem. Phys.* **20** 1493–1495
[5] Voitsekhovskii B, Mitrofanov V and Topchiyan M 1969 *Combust. Explos. Shock Waves* **5**(3) 267–273
[6] Brenner D W, Robertson D H, Elert M L and White C T 1993 *Phys. Rev. Lett.* **70** 2174-2177; 1996 *ibid.* **76** 2202
[7] For a review, see White C T, Swanson D R and Robertson D H 2001 *Chemical Dynamics in Extreme Environments* (London: World Scientific) Chap. 11 547–592
[8] Heim A J, Grønbech-Jensen N, Kober E M, Erpenbeck J J and Germann T C 2008 *Phys. Rev.* E **78**(4) 046709
[9] Zhakhovsky V V, Budzevich M M, Landerville A C, Oleynik I I and White C T submitted to *Phys. Rev.* E
[10] Zhakhovskii V V, Nishihara K and Anisimov S I 1997 *JETP Lett.* **66** 99–105
[11] Zhakhovsky V V, Budzevich M M, Oleynik I I and White C T 2011 *Phys. Rev. Lett.* **107** 135502
[12] Tsuboi N, Eto K and Hayashi A 2007 *Combust. Flame* **149** 144–161
[13] Anisimov S I, Zhakhovskii V V and Fortov V E 1997 *JETP Lett.* **65** 755–761
[14] Mott-Smith H M 1951 *Phys. Rev.* **82**(6) 885–892